

1 **Spatial transcriptomic landscape of the *Ciona* adult brain: functional zonalisation and**
2 **cellular composition in a sessile chordate brain and a novel insight into neural gland**
3 **function**

4 Xin Zeng^{1,2,3,†}, Fuki Gyoja^{4,†}, Ayana Maruo⁴, Nanako Okawa⁴, Ken-ichi Mizutani⁵, Yutaka Suzuki²,
5 Kenta Nakai^{1,2*} and Takehiro G. Kusakabe^{4*}

6 ¹ Human Genome Center, The Institute of Medical Science, The University of Tokyo, Tokyo, 108-
7 8639, Japan

8 ² Department of Computational Biology and Medical Sciences, The University of Tokyo, Kashiwa
9 277-8563, Japan

10 ³ Current address: Simons Center for Quantitative Biology, Cold Spring Harbor Laboratory, Cold
11 Spring Harbor, 11724, New York, US

12 ⁴ Institute for Integrative Neurobiology and Department of Biology, Konan University, Kobe, 658-
13 8501, Japan

14 ⁵ Graduate School of Pharmaceutical Sciences, Kobe Gakuin University, Kobe, 650-8586, Japan.

15

16 [†]These authors contributed equally to this work.

17 *To whom correspondence should be addressed. Email: knakai@ims.u-tokyo.ac.jp, [tgk@konan-
u.ac.jp](mailto:tgk@konan-
18 u.ac.jp)

19

20 **ABSTRACT**

21 The ascidian *Ciona* provides a key model for understanding the evolutionary origin of the
22 vertebrate brain. While the larval nervous system has been extensively characterized, the
23 molecular and cellular organization of the adult neural complex remains poorly defined. Here,
24 we generated spatial transcriptomic maps of the adult *Ciona* neural complex from three
25 individuals, with four serial sections per donor, using the 10x Visium platform. Clustering-based
26 analysis identified five major tissue domains, including the cerebral ganglion, neural gland,
27 ciliated funnel, neural gland duct/dorsal strand, and body wall muscle. To further refine spatial
28 resolution, we computationally reconstructed approximately 980 super-resolution gene
29 expression maps by integrating transcriptomic measurements with histological image features.
30 The super-resolution maps enabled precise delineation of molecular territories within the neural
31 complex. In the cerebral ganglion, high-resolution reconstruction revealed clear molecular
32 zonation, distinguishing the cortex and medulla. Within the cortex, the central region facing the
33 neural gland and anteroposterior distal regions showed distinct molecular properties. In the

34 neural gland, we identified coordinated enrichment of cell-cell interaction- and extracellular
35 matrix-related genes, suggesting specialized structural and physiological properties. We
36 propose that the neural gland play a pivotal role for the cerebral ganglion in maintaining
37 homeostasis, supporting development, and providing a signaling interface, which is reminiscent
38 of a primitive form of the choroid plexus and meninges found in vertebrates. Together, this
39 study provides the first spatially resolved transcriptomic atlas of the adult *Ciona* neural complex
40 and establishes a molecular framework for investigating functional regionalization and brain
41 evolution in chordates.

42

43 **INTRODUCTION**

44 The central nervous system (CNS) of the ascidian *Ciona*, one of the closest invertebrate relatives
45 of vertebrates, provides an important model for understanding the evolution of the vertebrate
46 brain ¹. For instance, a recent comparative study between *Ciona* larval brain and mouse
47 hypothalamus has provided insights into the evolutionary origin of vertebrate hypothalamic
48 neuroendocrine systems ². Although the larval nervous system of *Ciona* has been extensively
49 characterized at the transcriptomic and cellular levels ^{1,3-7}, the adult brain, which is referred to as
50 the neural complex, has received comparatively less attention. One reason for this is technical.
51 While it is relatively easy to analyse gene expression and function at the single-cell level in the
52 brain of ascidian larvae using transient transgenic techniques or whole-mount methods, it is
53 difficult to apply transgenic techniques or perform whole-mount analysis in the brain of adult
54 ascidians, which take several weeks to reach maturity after metamorphosis.

55 The *Ciona* neural complex consists primarily of the cerebral ganglion and the neural gland and is
56 thought to perform integrative and neuroendocrine-like functions ⁸. Cell lineage tracing studies
57 have revealed that the cerebral ganglion develops during metamorphosis from the neural
58 progenitor cells in the larval brain ^{9,10}. However, processes and mechanisms of the neural
59 complex development are still largely unknown. This is primarily due to a lack of information
60 regarding the types of cells that constitute the neural complex and their distribution. Recent
61 anatomical mapping studies have described the peripheral innervation architecture of the adult
62 nervous system ¹¹, and neuropeptidomic imaging has revealed regional neurochemical
63 organization within the cerebral ganglion ¹². However, a spatially resolved transcriptomic map
64 linking cellular identity, molecular programs, and anatomical structure across the adult neural
65 complex is still lacking. Recent advances in spatial transcriptomics enable genome-wide
66 measurement of gene expression while preserving tissue architecture ¹³. In addition,
67 computational approaches that integrate histological image features with transcriptomic
68 measurements can further refine spatial boundaries and reveal substructures beyond the native

69 resolution¹⁴. These advances provide an opportunity to systematically characterize the spatial
70 molecular architecture of the neural complex.

71 Here, we generated spatial transcriptomic data for the adult *Ciona* neural complex and applied
72 computational methods to improve spatial resolution. The resulting high-resolution spatial maps
73 enabled systematic identification of spatially restricted marker genes across the neural complex.
74 We further identified marker genes for the neural gland and three subregions of the cerebral
75 ganglion.

76

77 **RESULT**

78 **1. Spatial transcriptomic landscape of the adult brain of *Ciona***

79 The adult *Ciona* brain is located in the anterior region of the animal and is mainly composed of
80 two major structures: the cerebral ganglion and the neural gland (**Fig. 1A**). We collected brain
81 sections from three adult *Ciona* individuals using a balanced spatial replicate design (**Fig. 1B**).
82 For each individual, four serial sections from a comparable anatomical region were obtained and
83 distributed across different Visium slides. Histological images acquired during the Visium
84 workflow allowed clear identification of major anatomical features within the brain sections,
85 including the neural gland and cerebral ganglion (**Fig. 1C**). Spatial gene expression profiling of
86 these sections was performed using the 10x Genomics Visium platform. The resulting Visium
87 libraries produced approximately 3.9×10^8 to 4.4×10^8 reads per sample, with 414–532
88 spots detected under tissue. Across samples, the median UMI counts per spot ranged from
89 ~12,000 to ~20,000, and a median of ~3,300–4,200 genes were detected per spot
90 (**Supplementary Fig. 1A**). In total, 1,949 spots were retained for downstream analyses.

91 We performed downstream using Seurat v4¹⁵. To reduce technical variation across samples and
92 individuals, we applied canonical correlation analysis (CCA) to integrate Visium datasets prior to
93 clustering. After batch correction, spots from different samples and individuals were well mixed
94 in the integrated low-dimensional space, indicating effective removal of batch effects
95 (**Supplementary Figs. 1B and 1C**). We then performed graph-based community detection on
96 the integrated data and identified five clusters at the selected resolution (**Fig. 1D**, see Methods).
97 Similar clustering patterns were reproducibly observed across individuals and Visium slides,
98 indicating that the identified clusters were not driven by individual-specific effects (**Fig. 1E and**
99 **Supplementary Figs. 2A**).

100 **2. Tissue annotation for the adult brain of *Ciona***

101 We assigned each cluster to anatomical structures in the adult *Ciona* brain by combining
102 histological observations and differentially expressed genes. Specifically, we identified marker
103 genes for each spatial cluster based on differential expression analysis (see Methods), which
104 showed clear cluster-specific expression patterns (**Fig. 2A**). Clusters corresponding to the
105 cerebral ganglion and neural gland were identified based on their spatial correspondence to
106 these structures in histological images across sections. For clusters whose anatomical identity
107 could not be unambiguously determined from histology alone, we relied on complementary
108 lines of evidence. We annotated body wall muscle based on strong enrichment of Gene
109 Ontology (GO) terms related to muscle structure and contraction among its marker genes (**Fig.**
110 **2B**). In addition, we annotated the ciliated funnel by its anterior-most position and the
111 enrichment of GO terms associated with ciliary organization and motile cilia. Furthermore, we
112 annotated the neural gland duct together with the dorsal strand, based on its reproducible
113 spatial positioning relative to the cerebral ganglion and neural gland across individuals and
114 Visium slides.

115 **3. Construction of super-resolution gene maps of the *Ciona* brain**

116 Although the spatial clusters captured major anatomical structures of the *Ciona* brain, the
117 resolution of Visium transcriptomics data alone limited our ability to resolve finer substructures.
118 To overcome this limitation, we integrated transcriptomic information with spatial image
119 features derived from histological sections using Xfuse¹⁴. Compared with raw Visium spot-level
120 expression maps, Xfuse-inferred gene expression maps displayed sharper spatial boundaries and
121 more refined internal organization, enabling clearer delineation of anatomical domains (**Fig. 3A**).
122 In addition, these refined spatial patterns were independently supported by previously
123 published in situ hybridization data^{8,16}, in which the localization of *ci-galp* (KH.S618.6), *ci-ntlp-A*
124 (KH.C2.14), *ci-vfyl/l* (KH.C2.1145), *ci-lf* (KH.C10.27), and *vasopressin receptor* (KH.C9.885) signals
125 consistently showed enrichment in the cortical region of the cerebral ganglion and that of
126 *somatostatin receptor* (KH.C8.337) confined to the neural gland, matching the domains identified
127 by spatial transcriptomics (**Supplementary Figs. 3A-3C**). We then systematically generated
128 super-resolution gene expression maps for all cell-type-specific differentially expressed genes
129 using Xfuse, resulting in approximately 980 high-resolution expression maps in total (**Fig. 3B**).

130 **4. Identification of new marker genes for the neural gland**

131 Using super-resolution gene expression maps, we identified a set of new marker genes with
132 spatially restricted expression patterns for the neural complex. In the neural gland, 85 genes
133 showed highly consistent and confined enrichment within this region across individuals (**Fig. 3C**;
134 **Supplementary Table S1**). The list of these genes illuminates distinct physiological roles of this
135 organ. A number of genes are related to extracellular matrix (ECM), including KH.C1.1211
136 (laminin), KH.C5.562 (dystroglycan), KH.C8.476 (lysyl oxidase like 3), KH.C9.371 (discoidin domain

137 receptor tyrosine kinase 2), KH.C13.31 (secreted protein acidic and cysteine rich), KH.L87.44
138 (versican), KH.L139.15 (hemicentin-1), KH.C13.129 (sushi, von Willebrand factor type A, EGF and
139 pentraxin domain containing 1), KH.C1.707 (mucin 13), and KH.C1.1291 (matrix metalloproteinase
140 16). Another conspicuous feature is the expression of prospective neural support and axon
141 guidance molecules, such as KH.C12.72 (netrin 1), KH.C5.524 (netrin 4), KH.C5.490 (netrin
142 receptor unc-5), KH.L18.70 (neuregulin 2), KH.C11.251 (nerve growth factor receptor), and
143 KH.S749.1 (glial fibrillary acidic protein, GFAP). Transmembrane receptors and adhesion
144 molecules are also noticeable, including KH.C11.90/KH.C8.337 (somatostatin receptors),
145 KH.C2.341 (G-protein-coupled receptor 107), KH.C14.202 (insulin receptor related receptor),
146 KH.C9.149 (prostaglandin I2 receptor), KH.C9.260 (frizzled class receptor 5/8), KH.C14.562
147 (adhesion GPCR D1), KH.C14.88 (FAT atypical cadherin 1), and KH.C12.14 (cadherin 18). The
148 marker genes for the neural gland also include genes for solute carrier family (SLC) transporters
149 (KH.C7.199, KH.L4.19, KH.S215.18), calponin (KH.C4.559), and proteins involved in cell growth
150 and differentiation, such as KH.C2.605 (hedgehog interacting protein), KH.C2.957 (msh
151 homeobox), KH.C4.236 (Elf3/Ehf transcription factor), KH.C7.22 (ectodysplasin A), and KH.L112.16
152 (Jun/AP-1 transcription factor subunit). The coordinated enrichment of these molecules suggests
153 distinct cell–cell interaction and extracellular environment properties within the neural gland,
154 consistent with its proposed secretory and interface-related roles.

155 **5. Identification of new marker genes for the cerebral ganglion**

156 We next focused on the cerebral ganglion. The cerebral ganglion is divided into the cortex and
157 medulla ^{17,18}. The super-resolution gene expression maps revealed that spatial expression
158 patterns could be broadly classified into four major groups: i) uniformly expressed in the cortex
159 (cortex), ii) predominantly expressed in the central cortex region, particularly in the ventral
160 region facing the neural gland (central), iii) predominantly expressed in anterior and posterior
161 parts of the cortex (anteroposterior), and iv) predominantly expressed in the inner medulla
162 region (medulla). For the cortex (**Fig. 3D; Supplementary Table S2**), we identified marker genes
163 including KH.C7.92 (NMDA receptor), KH.C12.16 (carboxypeptidase E), KH.L128.2 (proprotein
164 convertase 2), KH.S761.6 (glutamate decarboxylase), KH.C6.11 (aminopeptidase O), KH.S618.6
165 (galanin-like neuropeptide precursor), KH.C8.904 (Dickkopf 3) and KH.C1.215 (acid sensing ion
166 channel subunit 1/2/3). Many of these genes are associated with the biogenesis of gamma-
167 aminobutyric acid (GABA) and neuropeptides, and synaptic function and proton-gated ion
168 channel activity, suggesting active neuronal signaling and peptide processing activities in this
169 region. For the central cortex domain (**Fig. 3E; Supplementary Table S3**), we identified marker
170 genes including KH.C1.421 (4-aminobutyrate aminotransferase, ABAT), KH.C1.498 (choline O-
171 acetyltransferase), KH.C12.218 (acetylcholine esterase), KH.C9.885 (vasopressin receptor),
172 KH.C1.1067 (neuronal calcium sensor 1), KH.C2.101 (synaptotagmin), KH.C5.389 (tachykinin
173 precursor), KH.L22.28 (type B GABA receptor), KH.C1.467 (μ -opioid/somatostatin/angiotensin

174 receptor-like), KH.S1051.1/KH.S1104.4 (gonadotropin-releasing hormone, GnRH, precursor) and
175 KH.C9.462 (voltage-gated Na⁺ channel). These genes suggest specialized neurotransmitter
176 response and synaptic vesicle release properties in this subregion. For the anteroposterior distal
177 regions (**Fig. 3F; Supplementary Table S4**), we identified marker genes including KH.C2.491
178 (golgin A4), KH.C4.437 (Ca²⁺/calmodulin-dependent protein kinase IV), KH.C6.106
179 (phosphodiesterase 4D interacting protein), KH.C3.474 (MAM domain containing
180 glycosylphosphatidylinositol anchor 2; MDGA2), and KH.C7.399 (calcitonin). For the medulla (**Fig.**
181 **3G; Supplementary Table S5**), we identified marker genes including KH.L55.2 and KH.C10.335
182 (calmodulin family members), KH.C9.150 (doublecortin-like and CAM kinase-like 2), KH.C8.892
183 (α -tubulin), KH.L116.85 (β -tubulin), and KH.C1.342 (voltage-gated Ca²⁺ channel). These genes are
184 related to calcium signaling and cytoskeletal structure, consistent with structural core and
185 regulatory function in the cerebral ganglion.

186

187 **DISCUSSION**

188 In this study, we present a spatially resolved transcriptomic atlas of the adult *Ciona* neural
189 complex. Clustering-based analysis defined the major tissue domains of the adult neural
190 complex, providing a comprehensive transcriptional framework for understanding its
191 organization and surrounding structures. In addition to the cerebral ganglion and neural gland,
192 the atlas also resolves adjacent tissues such as the ciliated funnel, the neural gland duct, and the
193 dorsal strand, offering a spatial molecular resource that may facilitate future studies of these
194 structures.

195 To further refine spatial resolution in adult tissues, we generated super-resolution gene
196 expression maps by integrating histological image features with spatial transcriptomic data. This
197 approach provides a scalable molecular reference that reduces reliance on gene-by-gene
198 anatomical screening. Based on the super-resolution gene expression maps, we identified
199 spatially restricted marker genes for both the neural gland and the cerebral ganglion. The neural
200 gland displays a distinct molecular signature consistent with specialized structural and secretory
201 functions, while the cerebral ganglion exhibits clear internal zonation, indicating functional
202 compartmentalization within this compact brain. These findings suggest that the spatial
203 organization of neuronal and neuroendocrine programs is already established in a simple
204 chordate nervous system. Previous studies have identified conserved molecular signatures
205 shared between *Ciona* and vertebrates in particular cell types, including photoreceptor-related
206 cells¹⁹ and hypothalamic neuroendocrine lineages². The atlas presented here extends these
207 efforts by providing a comprehensive spatial framework for comparing conserved molecular
208 signatures across species, thereby enabling systematic investigation of how regional
209 specialization of the vertebrate brain emerged during evolution.

210 Special attention has been paid to the neural gland due to its distinct anatomical features and
211 possible homology to vertebrate organs. The proposed homologous organs in vertebrates
212 include adenophypophysis^{20,21} and choroid plexus¹⁶. Various functions have been proposed for
213 the neural gland, including an endocrine organ²¹⁻²³, an excretory organ²⁴, an exocrine organ¹⁶,
214 a lymph producing organ²², an osmoregulatory organ^{16,25}, and an organ that mediates
215 regeneration of the cerebral ganglion^{26,27}. Despite these interests and studies, the physiological
216 and developmental roles of this organ remain elusive. Accordingly, only a few genes have been
217 identified as specifically expressed in the neural gland^{8,16}.

218 In the present study, we identified 85 neural gland-specific genes. These genes support some of
219 the previously proposed functions and homology of the neural gland. Expression of various SLC
220 transporters with calponin suggests its role in regulating chemical (ions, amino acids, and
221 peptides) and physical (pressure or flow of fluid) environment around the neural complex, or
222 acting as a selective barrier, similar to a blood-brain barrier of vertebrates. A osmoregulatory
223 role is also suggested by the expression of various GPCRs for the putative osmoregulatory
224 neuropeptides; some of these receptors are also expressed in the vertebrate choroid plexus¹⁶.
225 Deyts et al. (2006) proposed that the neural gland is an osmoregulatory organ and might be
226 homologous to the choroid plexus of vertebrates. Furthermore, expression of GFAP and neural
227 guidance cues (netrins, netrin receptors, and neuregulin 2) supports a proposed role of the
228 neural gland in development and regeneration of the cerebral ganglion. Our results are
229 compatible with this idea and further extend its neuroprotective and supportive roles, similar to
230 the blood-brain barrier of vertebrates. The richness of ECM proteins and putative protective and
231 instructive roles for the brain are also reminiscent of the meninges of vertebrates, especially the
232 pia mater, where the choroid plexus derive from. Thus, the neural gland may represent a
233 primitive form of the meninges-choroid plexus system in vertebrates.

234 Previously, the cortex and medulla are recognized as distinct regions in the cerebral ganglion
235^{17,18}. Our super-resolved gene maps identified four groups of gene expression patterns in the
236 cerebral ganglion: i) uniformly expressed in the cortex, ii) predominantly expressed in the central
237 cortex region, particularly in the cortex region facing the neural gland, iii) predominantly
238 expressed in the anterior and posterior parts of the cortex, and iv) predominantly expressed in
239 the medulla. Pan-cortex and central cortex genes include genes for the biogenesis of
240 neurotransmitters and neuropeptides, their receptors, and various proteins involved in synaptic
241 function, suggesting that the cortex contains a number of neurons and serves as the primary site
242 of neuronal activity. On the contrary, the anteroposterior distal regions of the cortex show a
243 distinct molecular signature in which proteins associated with neuronal and synaptic functions
244 are less prominent, suggesting a distinct molecular function of these regions. In the medulla,
245 genes for proteins involved in intracellular Ca²⁺ signaling are conspicuously expressed together
246 with microtubule components. Expression of these genes suggests the medulla serves as the

247 structural core of the cerebral ganglion and plays a regulatory role with active Ca²⁺ signaling,
248 which is reminiscent of astrocytes in the vertebrate brain. In summary, the present analysis
249 revealed previously unrecognized molecular heterogeneity in the cerebral ganglion, especially
250 within the cortex.

251 Several limitations should be acknowledged. First, the current spatial maps are derived from
252 spot-based measurements, and integration with single-cell RNA sequencing data from the adult
253 brain will be necessary to further refine cell-type-specific expression patterns. Such integration
254 would enable more precise delineation of cellular heterogeneity within each anatomical domain
255 ²⁸. Second, we did not perform extensive regulatory network analysis. In *Ciona*, widespread
256 trans-splicing complicates transcript-level assignment and regulatory inference ²⁹, posing
257 challenges for conventional gene regulatory network reconstruction. Future studies combining
258 improved transcript annotation, single-cell data, and perturbation experiments will be essential
259 for dissecting regulatory mechanisms underlying the spatial programs described here.

260

261 **DATA AVAILABILITY**

262 FASTQ data from this study can be downloaded from GEO database (GSE327796). Processed
263 data can be downloaded from figshare (<https://doi.org/10.6084/m9.figshare.31915545>). Codes
264 generated for this project are available on GitHub (https://github.com/xzengComBio/Ciona_ST).

265

266 **AUTHOR CONTRIBUTIONS**

267 Conceptualization, X.Z., F.G., T.G.K., and K.N.; Visium Data Acquisition, A.M., N.O., K.M., T.G.K.,
268 and Y.S.; Data Curation, X.Z. and T.G.K.; Formal Analysis, X.Z.; Investigation, X.Z., F.G., A.M., and
269 T.G.K.; Writing – Original Draft, X.Z., F.G., and T.G.K.; Writing – Review & Editing, X.Z., F.G., T.G.K.,
270 and K.N.; Funding Acquisition, T.G.K. Y.S., and K.N.; Resources, K.M., Y.S., T.G.K., and K.N.;
271 Supervision, T.G.K. and K.N.

272

273 **ACKNOWLEDGEMENTS**

274 We thank the National BioResource Project of MEXT and all members of the Maizuru Fisheries
275 Research Station and Yutaka Satou Lab of Kyoto University and the Misaki Marine Biological
276 Station and Manabu Yoshida Lab of the University of Tokyo for providing us with *C. intestinalis*
277 type A adults. We also thank the Graduate School of Maritime Sciences, Kobe University, for

278 generously allowing us to collect *C. intestinalis* type A on the campus. Computational resources
279 were provided by the supercomputer system SHIROKANE at the Human Genome Center,
280 Institute of Medical Science, the University of Tokyo.

281

282 **FUNDING**

283 KAKENHI Grants-in-Aid for Scientific Research [23K27185, 23H02492, 22K06189, 21K19280] from
284 the Japan Society for the Promotion of Science; Hirao Taro Foundation of KONAN GAKUEN for
285 Academic Research and the Takeda Science Foundation [2015021209, in part]; XZ was supported
286 by JST SPRING (JPMJSP2108).

287

288 **CONFLICT OF INTEREST**

289 The authors declare that they have no competing interests.

290

291

292 **REFERENCES**

- 293 1. Kusakabe, T.G. (2017). Identifying vertebrate brain prototypes in deuterostomes. In *Brain Evolution by*
294 *Design: From Neural Origin to Cognitive Architecture* (Springer), pp. 153–186.
- 295 2. Lemaire, L.A., Cao, C., Yoon, P.H., Long, J., and Levine, M. (2021). The hypothalamus predates the
296 origin of vertebrates. *Sci. Adv.* 7, eabf7452. <https://doi.org/10.1126/sciadv.abf7452>.
- 297 3. Horie, T., Nakagawa, M., Sasakura, Y., and Kusakabe, T.G. (2009). Cell type and function of neurons in
298 the ascidian nervous system. *Dev Growth Differ* 51, 207–220. [https://doi.org/10.1111/j.1440-](https://doi.org/10.1111/j.1440-169X.2009.01105.x)
299 [169X.2009.01105.x](https://doi.org/10.1111/j.1440-169X.2009.01105.x).
- 300 4. Ryan, K., Lu, Z., and Meinertzhagen, I.A. (2016). The CNS connectome of a tadpole larva of *Ciona*
301 *intestinalis* (L.) highlights sidedness in the brain of a chordate sibling. *eLife* 5, e16962.
302 <https://doi.org/10.7554/eLife.16962>.
- 303 5. Ryan, K., Lu, Z., and Meinertzhagen, I.A. (2017). Circuit Homology between Decussating Pathways in
304 the *Ciona* Larval CNS and the Vertebrate Startle-Response Pathway. *Current Biology* 27, 721–728.
305 <https://doi.org/10.1016/j.cub.2017.01.026>.
- 306 6. Cao, C., Lemaire, L.A., Wang, W., Yoon, P.H., Choi, Y.A., Parsons, L.R., Matese, J.C., Wang, W., Levine, M.,
307 and Chen, K. (2019). Comprehensive single-cell transcriptome lineages of a proto-vertebrate. *Nature*
308 571, 349–354. <https://doi.org/10.1038/s41586-019-1385-y>.
- 309 7. Sharma, S., Wang, W., and Stolfi, A. (2019). Single-cell transcriptome profiling of the *Ciona* larval brain.
310 *Developmental Biology* 448, 226–236. <https://doi.org/10.1016/j.ydbio.2018.09.023>.

- 311 8. Kawada, T., Ogasawara, M., Sekiguchi, T., Aoyama, M., Hotta, K., Oka, K., and Satake, H. (2011).
312 Peptidomic Analysis of the Central Nervous System of the Protochordate, *Ciona intestinalis*:
313 Homologs and Prototypes of Vertebrate Peptides and Novel Peptides. *Endocrinology* 152, 2416–2427.
314 <https://doi.org/10.1210/en.2010-1348>.
- 315 9. Horie, T., Shinki, R., Ogura, Y., Kusakabe, T.G., Satoh, N., and Sasakura, Y. (2011). Ependymal cells of
316 chordate larvae are stem-like cells that form the adult nervous system. *Nature* 469, 525–528.
317 <https://doi.org/10.1038/nature09631>.
- 318 10. Todorov, L.G., Oonuma, K., Kusakabe, T.G., Levine, M.S., and Lemaire, L.A. (2024). Neural crest lineage
319 in the protovertebrate model *Ciona*. *Nature* 635, 912–916. [https://doi.org/10.1038/s41586-024-](https://doi.org/10.1038/s41586-024-08111-7)
320 [08111-7](https://doi.org/10.1038/s41586-024-08111-7).
- 321 11. Osugi, T., Sasakura, Y., and Satake, H. (2017). The nervous system of the adult ascidian *Ciona*
322 *intestinalis* Type A (*Ciona robusta*): Insights from transgenic animal models. *PLoS ONE* 12, e0180227.
323 <https://doi.org/10.1371/journal.pone.0180227>.
- 324 12. Osugi, T., Shiraishi, A., Sasakura, Y., Sugahara, K., Yamagaki, T., Yamamoto, T., and Satake, H. (2025).
325 Two- and three-dimensional neuropeptidomic landscape in the central nervous system of an
326 invertebrate chordate, *Ciona robusta*. *iScience* 28, 113413. <https://doi.org/10.1016/j.isci.2025.113413>.
- 327 13. Ståhl, P.L., Salmén, F., Vickovic, S., Lundmark, A., Navarro, J.F., Magnusson, J., Giacomello, S., Asp, M.,
328 Westholm, J.O., Huss, M., et al. (2016). Visualization and analysis of gene expression in tissue sections
329 by spatial transcriptomics. *Science* 353, 78–82. <https://doi.org/10.1126/science.aaf2403>.
- 330 14. Bergenstråhle, L., He, B., Bergenstråhle, J., Abalo, X., Mirzazadeh, R., Thrane, K., Ji, A.L., Andersson, A.,
331 Larsson, L., Stakenborg, N., et al. (2021). Super-resolved spatial transcriptomics by deep data fusion.
332 *Nat Biotechnol*, 1–4. <https://doi.org/10.1038/s41587-021-01075-3>.
- 333 15. Stuart, T., Butler, A., Hoffman, P., Hafemeister, C., Papalexi, E., Mauck, W.M., Hao, Y., Stoeckius, M.,
334 Smibert, P., and Satija, R. (2019). Comprehensive Integration of Single-Cell Data. *Cell* 177, 1888-
335 1902.e21. <https://doi.org/10.1016/j.cell.2019.05.031>.
- 336 16. Deyts, C., Casane, D., Vernier, P., Bourrat, F., and Joly, J. (2006). Morphological and gene expression
337 similarities suggest that the ascidian neural gland may be osmoregulatory and homologous to
338 vertebrate periventricular organs. *Eur J of Neuroscience* 24, 2299–2308.
339 <https://doi.org/10.1111/j.1460-9568.2006.05073.x>.
- 340 17. Koyama, H., and Kusunoki, T. (1993). Organization of the cerebral ganglion of the colonial ascidian
341 *Polyandrocarpa misakiensis*. *J of Comparative Neurology* 338, 549–559.
342 <https://doi.org/10.1002/cne.903380405>.
- 343 18. Dahlberg, C., Auger, H., Dupont, S., Sasakura, Y., Thorndyke, M., and Joly, J.-S. (2009). Refining the
344 *Ciona intestinalis* Model of Central Nervous System Regeneration. *PLoS ONE* 4, e4458.
345 <https://doi.org/10.1371/journal.pone.0004458>.
- 346 19. Zeng, X., Gyoja, F., Cui, Y., Loza, M., Kusakabe, T.G., and Nakai, K. (2024). Comparative single-cell
347 transcriptomic analysis reveals putative differentiation drivers and potential origin of vertebrate retina.
348 *NAR Genomics and Bioinformatics* 6, lqae149. <https://doi.org/10.1093/nargab/lqae149>.
- 349 20. Gorbman, A. (1995). Olfactory origins and evolution of the brain pituitary endocrine system: facts and
350 speculation. *General and Comparative Endocrinology* 97, 171–178.
- 351 21. Pestarino, M. (1984). Immunocytochemical demonstration of prolactin-like activity in the neural gland
352 of the ascidian *Styela plicata*. *General and Comparative Endocrinology* 54, 444–449.
- 353 22. Herdman, W.A. (1883). The hypophysis cerebri in Tunicata and Vertebrata. *Nature* 28, 284–286.
- 354 23. Willey, A., and Lond, B. (1893). Studies on the Protochordata. *Quat. J. Micr. Sci.* 35, 295–333.
- 355 24. Ruppert, E.E., and Smith, P.R. (1988). THE FUNCTIONAL ORGANIZATION OF FILTRATION NEPHRIDIA.
356 *Biological Reviews* 63, 231–258. <https://doi.org/10.1111/j.1469-185X.1988.tb00631.x>.

- 357 25. Ruppert, E.E. (1990). Structure, ultrastructure and function of the neural gland complex of *Ascidia*
358 *interrupta* (Chordata, Ascidiacea): clarification of hypotheses regarding the evolution of the vertebrate
359 anterior pituitary. *Royal Swedish Academy of Sciences* 71, 135–149.
- 360 26. Medina, B.N.S.P., Santos De Abreu, I., Cavalcante, L.A., Silva, W.A.B., Da Fonseca, R.N., Allodi, S., and De
361 Barros, C.M. (2015). 3-acetylpyridine-induced degeneration in the adult ascidian neural complex:
362 Reactive and regenerative changes in glia and blood cells. *Developmental Neurobiology* 75, 877–893.
363 <https://doi.org/10.1002/dneu.22255>.
- 364 27. De Abreu, I.S., Wajsenzon, I.J.R., Dias, J.C., Allodi, S., and Monteiro-de-Barros, C. (2022). Central
365 nervous system regeneration in ascidians: cell migration and differentiation. *Cell Tissue Res* 390, 335–
366 354. <https://doi.org/10.1007/s00441-022-03677-y>.
- 367 28. Rao, A., Barkley, D., França, G.S., and Yanai, I. (2021). Exploring tissue architecture using spatial
368 transcriptomics. *Nature* 596, 211–220. <https://doi.org/10.1038/s41586-021-03634-9>.
- 369 29. Yokomori, R., Kusakabe, T.G., and Nakai, K. (2024). Characterization of *trans*-spliced chimeric RNAs:
370 insights into the mechanism of *trans*-splicing. *NAR Genomics and Bioinformatics* 6, lqae067.
371 <https://doi.org/10.1093/nargab/lqae067>.
- 372 30. Satou, Y., Mineta, K., Ogasawara, M., Sasakura, Y., Shoguchi, E., Ueno, K., Yamada, L., Matsumoto, J.,
373 Wasserscheid, J., Dewar, K., et al. (2008). Improved genome assembly and evidence-based global gene
374 model set for the chordate *Ciona intestinalis*: new insight into intron and operon populations.
375 *Genome Biol* 9, R152. <https://doi.org/10.1186/gb-2008-9-10-r152>.
- 376 31. Lause, J., Berens, P., and Kobak, D. (2021). Analytic Pearson residuals for normalization of single-cell
377 RNA-seq UMI data. *Genome Biol* 22, 258. <https://doi.org/10.1186/s13059-021-02451-7>.
- 378 32. Dardaillon, J., Dauga, D., Simion, P., Faure, E., Onuma, T.A., DeBiase, M.B., Louis, A., Nitta, K.R., Naville,
379 M., Besnardeau, L., et al. (2019). ANISEED 2019: 4D exploration of genetic data for an extended range
380 of tunicates. *Nucleic Acids Research*, gkz955. <https://doi.org/10.1093/nar/gkz955>.
- 381 33. Xu, S., Hu, E., Cai, Y., Xie, Z., Luo, X., Zhan, L., Tang, W., Wang, Q., Liu, B., Wang, R., et al. (2024). Using
382 clusterProfiler to characterize multiomics data. *Nat Protoc* 19, 3292–3320.
383 <https://doi.org/10.1038/s41596-024-01020-z>.

384
385

386 **MATERIALS AND METHODS**

387 **Biological materials**

388 Mature adults of *Ciona intestinalis* type A were provided by the Maizuru Fisheries Research
389 Station of Kyoto University and by the Misaki Marine Biological Station of the University of
390 Tokyo through the National Bio Resource Project (NBRP) of the Ministry of Education, Culture,
391 Sports, Science and Technology of Japan (MEXT). These were maintained in indoor tanks of
392 artificial seawater (ASW) (Marine Art BR; Tomita Pharmaceutical, Tokushima, Japan) at 17–20°C.

393

394 **Tissue preparation and VISIUM sequencing library construction**

395 *Ciona* whole brains were surgically dissected from mature adult individuals, embedded in
396 Tissue-Tek OCT compound (Sakura Finetek, Tokyo, Japan), and sectioned at 10- μ m thickness
397 using a cryostat (HM525, Microm). Tissue fixation and staining were as described in the

398 Methanol Fixation, H&E Staining & Imaging for Visium Spatial Protocols (10X Genomics;
399 #CG000160 Rev C). Tissue permeabilization optimization was performed using Visium Spatial
400 Tissue Optimization Slide & Reagent Kit (10 \times Genomics, #1000193) according to the Visium
401 Spatial Tissue Optimization User Guide Rev B (10 \times Genomics, #CG000238). The optimal tissue
402 permeabilization time for *Ciona* brains was determined as 12 min. The optimized condition was
403 then used for Visium Spatial Gene Expression library preparation. The four capture areas on the
404 Visium Gene Expression Slide (#2,000,233) contained serial sections from an embedded brain
405 block, including three brains from different individuals. When embedded, the brain tissues were
406 aligned in the same direction so that each capture area contained three sagittal brain sections.
407 Each capture area of the Visium Gene Expression Slide contained approximately 5000 barcoded
408 spots of 55 μ m in diameter (100- μ m center-to-center spacing between spots). The sequencing
409 library was prepared using Visium Spatial Gene Expression Slide & Reagent Kit (10 \times Genomics,
410 #1000184) according to the Visium Spatial Gene Expression User Guide Rev C (10X Genomics,
411 #CG000239) and sequenced on a NovaSeq 6000 system (Illumina). Sequencing was performed
412 with the recommended protocol (read 1: 28 cycles; i7 index read: 10 cycles; i5 index read: 10
413 cycles; and read 2: 90 cycles), yielding between 391 million and 440 million sequenced reads.

414

415 **Mapping**

416 Sequencing output was processed through the Space Ranger 1.3.1 count function using default
417 parameters. Reads were quantified using the KH2013 reference genome provided by the Ghost
418 Database³⁰. The raw count matrices were subsequently imported into R and subjected to
419 analysis using the Seurat 4 package¹⁵. The data were log normalized and scaled by the
420 SCTransform function³¹, followed by batch effect correction using canonical correlation analysis.
421 The corrected data were scaled for the principal component analysis (PCA). The corrected data
422 was used for clustering based on a shared nearest-neighbor modularity optimization-based
423 clustering algorithm with default parameters and resolutions at 0.2. Non-linear dimensionality
424 reduction was conducted using UMAP.

425 We performed Gene Ontology enrichment analysis for cluster-specific marker genes identified
426 from spatial transcriptomic data using a custom *Ciona* GO annotation derived from the Aniseed
427 GAF file³². Enrichment of Biological Process terms was tested with clusterProfiler³³, and the top-
428 enriched GO terms for each cluster were visualized using dot plots.

429

430 **Generation of super-resolution gene maps**

431 We used xfuse¹⁴ to generate high resolution gene expression map for marker genes. First, the
432 coordinates on each brain section were extracted from the original “tissue_positions_list.csv” file.
433 Then, the transcriptomics and image information for each brain section were extracted using
434 xfuse convert Visium function with a scale value setting to 0.2. Finally, the separated 12
435 transcriptomics and image section were train by the xfuse model using the xfuse run function via
436 Nvidia V100 GPU. The convergence of the model was achieved following a computational
437 duration of approximately 7 hours.

438

439

440

441 **FIGURES LEGENDS**

442 **Figure 1 Spatial transcriptomic landscape of the adult *Ciona* brain**

443 **A** Schematic illustration of the adult *Ciona* neural complex (adapted from ¹¹), highlighting the
444 two main brain structures, the cerebral ganglion and the neural gland. Orientation is indicated
445 by anterior–posterior (A–P) and dorsal–ventral (D–V) axes. **B** Experimental design for spatial
446 transcriptomics. Brain tissues from three adult individuals were sectioned serially, with four
447 sections per individual distributed across Visium slides. **C** Representative histological image from
448 the Visium workflow showing anatomical identification of the cerebral ganglion and neural
449 gland. The example shown is donor 3, a section from slide 2. **D** UMAP plots of all transcriptomic
450 spots colored by annotated tissues. **E** Spatial mapping of cell types onto tissue sections.

451

452 **Figure 2 Annotation of clusters in the adult brain of *Ciona***

453 **A** Heatmap showing scaled expression levels of representative marker genes across all tissue
454 types. **B** Gene Ontology (GO) enrichment analysis of marker genes for body wall muscle, ciliated
455 funnel, and neural gland duct/dorsal strand.

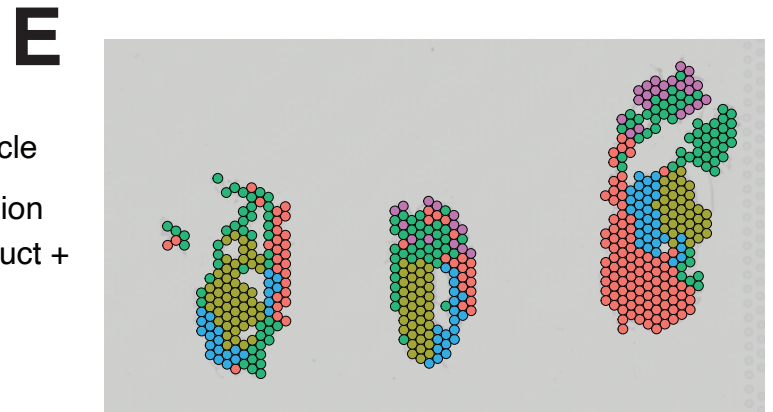
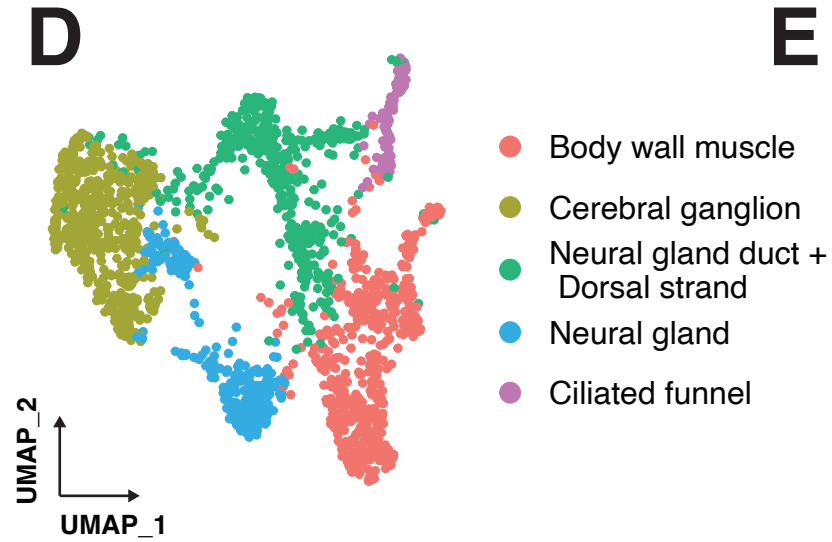
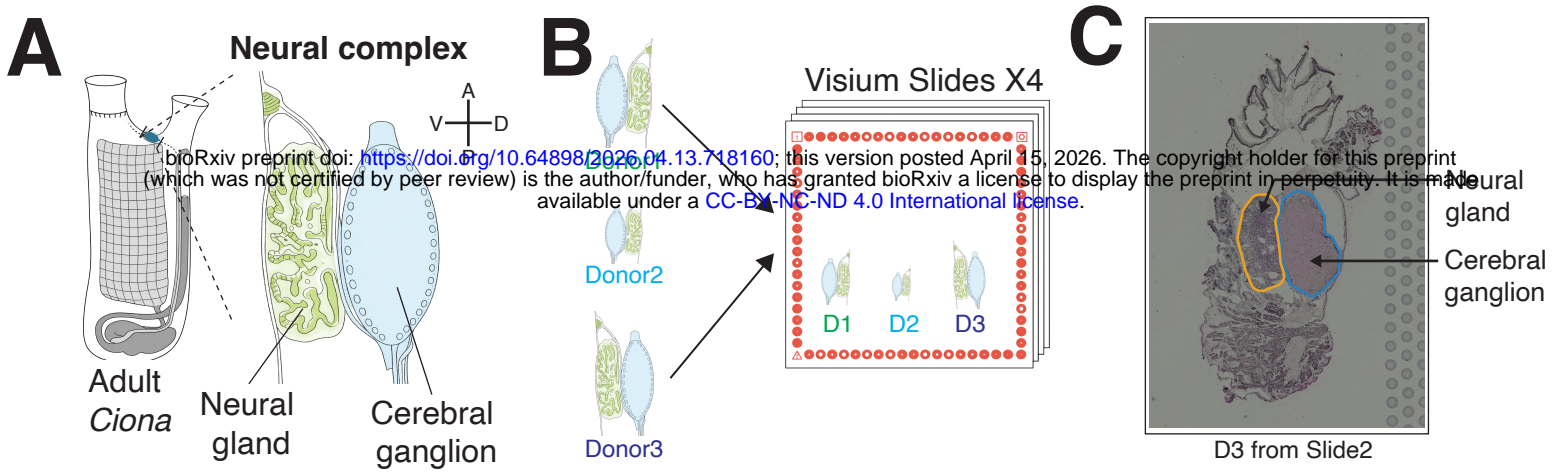
456

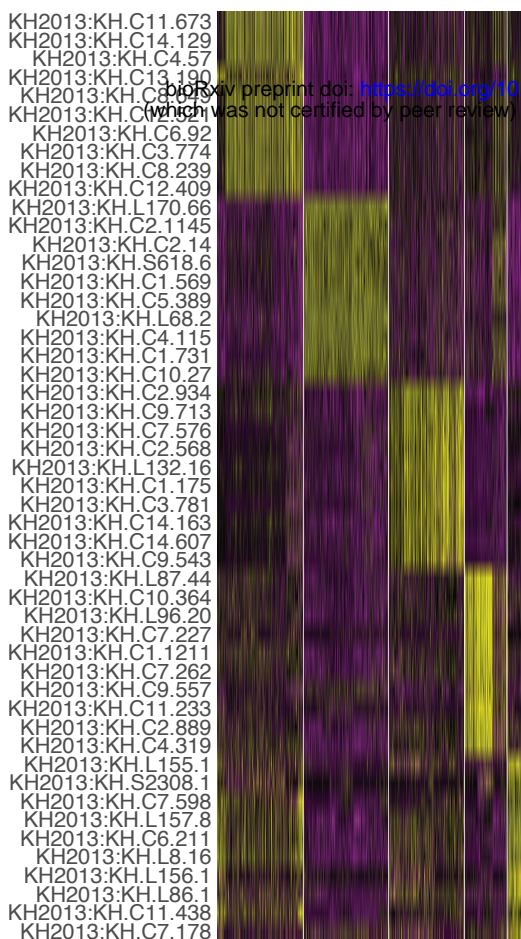
457 **Figure 3 Super-resolution spatial gene maps reveal region-specific marker genes in the 458 adult *Ciona* neural complex.**

459 **A** Representative examples of raw Visium spot-level expression maps and corresponding Xfuse-
460 inferred super-resolution maps for selected genes. **B** Number of genes generated by Xfuse for
461 each major anatomical cluster. **C–G** Super-resolution expression maps of representative marker

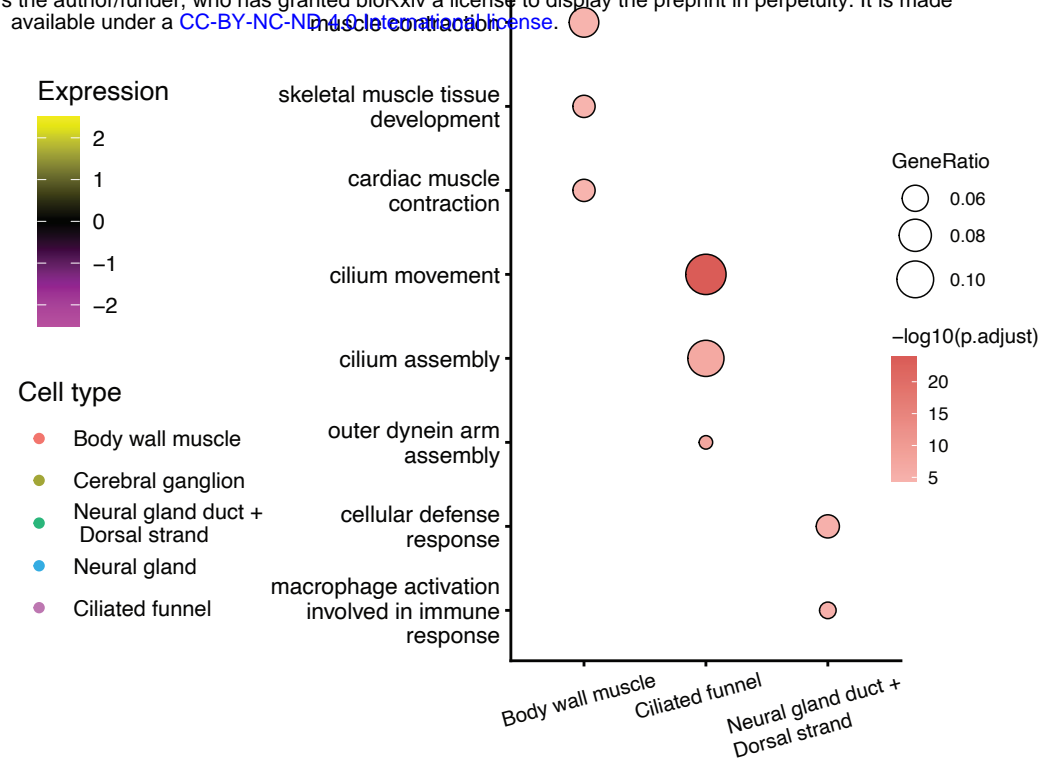
462 genes enriched in the neural gland (**C**) and different regions of the neural gland (pan-cortex, **D**;
463 central cortex, **E**; anteroposterior cortex, **F**; medulla, **G**).

464



A**B**

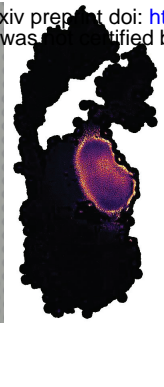
bioRxiv preprint doi: <https://doi.org/10.64898/2026.04.13.718160>; this version posted April 15, 2026. The copyright holder for this preprint (which was not certified by peer review) is the author/funder, who has granted bioRxiv a license to display the preprint in perpetuity. It is made available under a [CC-BY-NC-ND 4.0 International license](https://creativecommons.org/licenses/by-nc-nd/4.0/).



A**KH.C1.215**

Raw

Inferred

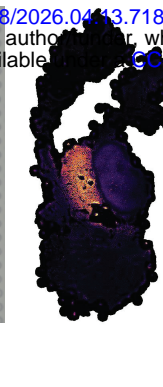


1 3

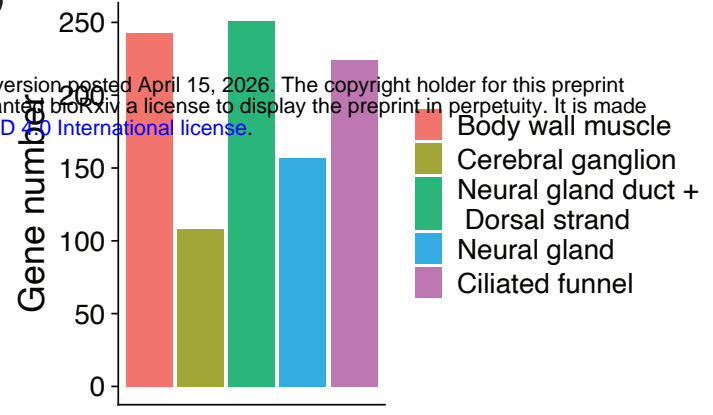
KH.C1.14

Raw

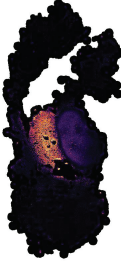
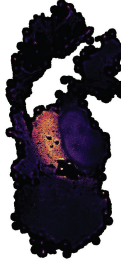
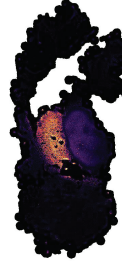
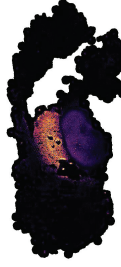
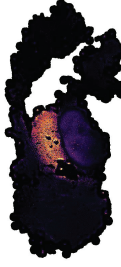
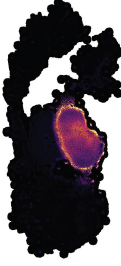
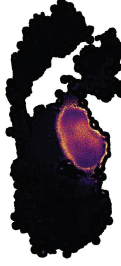
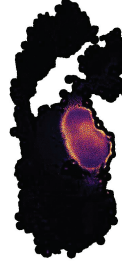
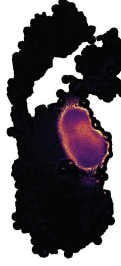
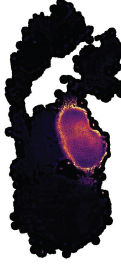
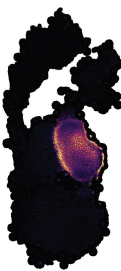
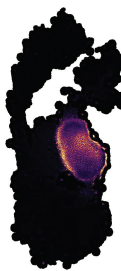
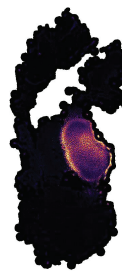
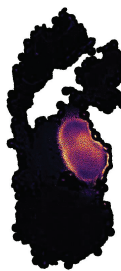
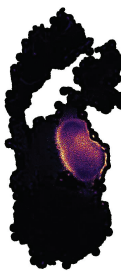
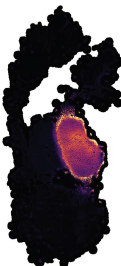
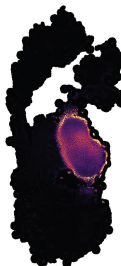
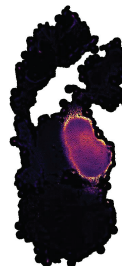
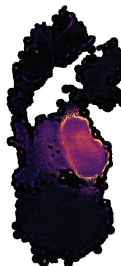
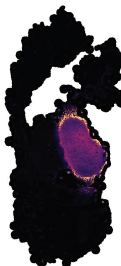
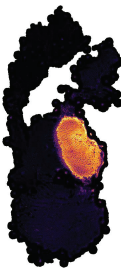
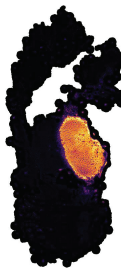
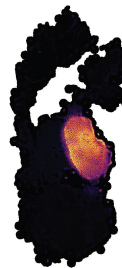
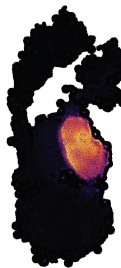
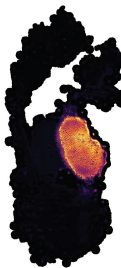
Inferred



0 2

B

Body wall muscle
Cerebral ganglion
Neural gland duct +
Dorsal strand
Neural gland
Ciliated funnel

C**Neural gland**KH.C14.562
Adhesion GPCR D1KH.C14.88
Fat1, atypical cadherinKH.C12.14
Cadherin-14/18KH.C1.707
Mucin 13KH.C1.1211
Laminin α 2**D****Cerebral ganglion (Cortex)**KH.C7.92
NMDA receptorKH.C12.16
Carboxypeptidase EKH.L128.2
Proteinase 2KH.C8.904
Dickkopf 3KH.S761.6
Glutamate decarboxylase**E****Cerebral ganglion (Central)**KH.C12.218
Acetylcholine esteraseKH.C9.885
Vasopressin receptorKH.C2.101
SynaptotagminKH.C1.467
Angiotensin receptorKH.C9.462
Voltage-gated Na⁺ channel**F****Cerebral ganglion (Anteroposterior)**KH.C2.491
Golgin A4KH.C3.474
MDGA2KH.C4.437
CaMKIVKH.C6.106
PDE4D interacting proteinKH.C7.399
Calcitonin**G****Cerebral ganglion (Medulla)**KH.L55.2
CalmodulinKH.C10.335
CalmodulinKH.C9.150
CAM kinase-like 2KH.C8.892
 α -tubulinKH.C1.342
Voltage-gated Ca²⁺ channel

bioRxiv preprint doi: <https://doi.org/10.64898/2026.04.13.718160>; this version posted April 15, 2026. The copyright holder for this preprint (which was not certified by peer review) is the author/funder, who has granted bioRxiv a license to display the preprint in perpetuity. It is made available under aCC-BY-NC-ND 4.0 International license.